

# Three-neutron resonance study using transition operators

A. Deltuva\*

*Institute of Theoretical Physics and Astronomy, Vilnius University, Saulėtekio al. 3, LT-10257 Vilnius, Lithuania*  
(Received December 27, 2017)

**Background:** Existing bound-state type calculations of three-neutron resonances yield contradicting results.

**Purpose:** A direct study of the three-neutron continuum using rigorous scattering equations with realistic potentials and search for possible resonances is aimed.

**Methods:** Faddeev-type integral equations for three-neutron transition operators are solved in the momentum-space partial-wave framework. The evolution of resonances is studied by enhancing the strength of the two-neutron interaction in partial waves with nonzero orbital momentum.

**Results:** Calculated three-neutron transition operators exhibit resonant behavior for sufficiently large enhancement factors; pole trajectories in the complex-energy energy plane are extracted from their energy dependence. However, the resonant behavior completely disappears for the physical interaction strength.

**Conclusions:** There are no physically observable three-neutron resonant states consistent with presently accepted interaction models.

PACS numbers: 21.30.-x, 21.45.-v

## I. INTRODUCTION

After a possible experimental observation of the four-neutron ( $4n$ ) resonance [1], a number of theoretical studies of multineutron systems emerged [2–5]. Their conclusions are, however, quite contradicting, even for the simplest three-neutron ( $3n$ ) system. While earlier studies [6, 7] based on the complex-scaled Faddeev equation found no  $3n$  resonances that could be physically observable, a recent work [4] predicted a  $3n$  resonance about 1 MeV above the threshold that should be potentially measurable. However, the latter studies relied on bound-state type calculations with extrapolation to the continuum. To shed more light on the possible existence and observability of the  $3n$  resonance, a direct study of the  $3n$  continuum using rigorous scattering equations is the aim of the present work. The integral equation formulation of the scattering theory for transition operators realized in the momentum-space partial-wave framework will be used. An important advantage of the direct continuum approach is its ability to estimate not only the resonance position but also its effect on scattering amplitudes that lead to observables in collision processes.

Section II describes three-particle scattering equations and some details of calculations whereas Sec. III reports results for a number of interaction models. The conclusions are presented in Sec. IV.

## II. THEORY

Faddeev equations for three-particle transition operators in the version proposed by Alt, Grassberger, and Sandhas (AGS) [8] have been extensively used for the description of the nucleon-deuteron scattering [9–11]. Using

the odd-man-out notation, the multichannel transition operators  $U_{\beta\alpha}$  satisfy the integral equations

$$U_{\beta\alpha} = \bar{\delta}_{\beta\alpha} G_0^{-1} + \sum_{\gamma} \bar{\delta}_{\beta\gamma} t_{\gamma} G_0 U_{\gamma\alpha} \quad (1a)$$

or, equivalently,

$$U_{\beta\alpha} = \bar{\delta}_{\beta\alpha} G_0^{-1} + \sum_{\gamma} U_{\beta\gamma} G_0 t_{\gamma} \bar{\delta}_{\gamma\alpha}. \quad (1b)$$

Here  $\bar{\delta}_{\beta\alpha} = 1 - \delta_{\beta\alpha}$ ,  $G_0 = (E + i0 - H_0)^{-1}$  is the free resolvent at the available three-particle energy  $E$  in the center-of-mass (c.m.) frame,  $H_0$  is the free Hamiltonian for the relative motion, and

$$t_{\gamma} = v_{\gamma} + v_{\gamma} G_0 t_{\gamma} \quad (2)$$

is the two-particle transition for the pair  $\gamma$  with  $v_{\gamma}$  being the corresponding potential. The sums over the spectator (pair) label  $\gamma$  in Eqs. (1) run from 1 to 3, thereby coupling only components corresponding to spectator + pair partitions. In the  $3n$  system there are no bound pairs, the only possible reaction is the elastic scattering of three free particles ( $3 \rightarrow 3$  process) whose operator can be obtained from  $U_{\beta\alpha}$  with  $\alpha, \beta = 1, 2, 3$  via the quadrature

$$U_{00} = \sum_{\alpha} t_{\alpha} + \sum_{\beta\alpha} t_{\beta} G_0 U_{\beta\alpha} G_0 t_{\alpha}. \quad (3)$$

For identical particles the system (1a) reduces to a single equation for the symmetrized transition operator

$$U = P G_0^{-1} + P t G_0 U \quad (4)$$

with the two-particle transition operator  $t$  for the representative pair 1 and  $P = P_{12} P_{23} + P_{13} P_{23}$ ,  $P_{\beta\alpha}$  being the permutation operator of particles  $\alpha$  and  $\beta$ ; the basis states must be antisymmetric only under the exchange of

\* arnoldas.deltuva@tfai.vu.lt

the neutrons within the pair. It is convenient to introduce an auxiliary Faddeev operator  $T = tG_0UG_0t$  obeying the integral equation

$$T = tG_0Pt + tG_0PT \quad (5)$$

since it is more directly related to the  $3 \rightarrow 3$  transition operator

$$U_{00} = (1 + P)t(1 + P) + (1 + P)T(1 + P). \quad (6)$$

The first term describes the two-neutron ( $nn$ ) scattering with the remaining one being a spectator and therefore does not correspond to a genuine three-particle process. Thus, for the investigation of the  $3n$  dynamics and possible resonances one should study the behavior of operators  $U$  or  $T$ , not  $U_{00}$ .

The AGS equations (4) and (5) are solved in the momentum-space. After the partial-wave decomposition they become a system of integral equations with two continuous variables, the magnitudes of the Jacobi momenta for the pair  $\mathbf{p} = (\mathbf{k}_2 - \mathbf{k}_3)/2$  and for the spectator  $\mathbf{q} = (2\mathbf{k}_1 - \mathbf{k}_2 - \mathbf{k}_3)/3$  where  $\mathbf{k}_\alpha$  are the individual momenta. The associated orbital angular momenta  $L$  and  $l$  together with neutron spins  $s_\alpha = \frac{1}{2}$ , through intermediate angular momenta  $s, j$ , and  $S_q$ , are coupled to the total angular momentum  $J$  with the projection  $M$ , resulting in the basis states  $|pq\nu\rangle = |pq(l\{L(s_2s_3)s\}j s_1)S_q JM\rangle$  with the total parity  $\Pi = (-1)^{L+l}$  where  $\nu$  abbreviates all discrete quantum numbers. Due to the antisymmetry condition only even  $(L+s)$  states are considered. The results are well converged by including two-neutron states with total angular momentum  $j < 3$ , i.e.,  $^1S_0, ^3P_0, ^3P_1, ^3P_2, ^3F_2$ , and  $^1D_2$  in the usual spectroscopic  $^{2s+1}L_j$  notation.

The numerical solution technique, including also the treatment of kernel singularities, is taken over from Ref. [12]. However, when studying the resonant behavior of transition operators one has to avoid special kinematic situations where already the on-shell driving term  $\langle p'q'\nu'|tG_0Pt|pq\nu\rangle$  in Eq. (5) becomes singular due to kinematic reasons and leads to divergences in  $\langle p'q'\nu'|T|pq\nu\rangle$  for particular combinations of initial and final momenta, i.e., for  $p'^2 + 3q'^2/4 = p^2 + 3q^2/4 = mE$  and  $q'^2 + q^2 \pm qq' = mE$ , with  $m$  being the neutron mass. In fact, such a situation corresponds to a free (on-shell) scattering of two-neutrons followed by a free scattering of two-neutrons within another pair, and therefore may be considered as a non-genuine three-particle reaction. In contrast, the  $3n$  resonance, corresponding to the pole of  $T$  and  $U$  in the complex-energy plane, manifests itself in *all* matrix elements of these transition operators, also fully off-shell. In the vicinity of the pole  $E_r - i\Gamma/2$  the transition operator in the corresponding  $J^\Pi$  state can be expanded in series

$$T_{J^\Pi} = \sum_{n=-1}^{\infty} \tilde{T}_{J^\Pi}^{(n)} (E - E_r + i\Gamma/2)^n \quad (7)$$

and well approximated by few lowest terms while higher-order terms yield negligible contribution.

Such a resonant behavior (or its absence) will be demonstrated using three types of initial and final states differing in their momentum distributions:

(1) q-state: on-shell state with  $p = 0$  and  $q = q_m = \sqrt{4mE/3}$ ; vanishing momentum  $p$  implies  $^1S_0$  state for the pair while  $l$  takes one of  $J \pm \frac{1}{2}$  values consistent with total parity;

(2) p-state: on-shell state with  $p = p_m = \sqrt{mE}$  and  $q = 0$ ; the second condition implies  $l = 0$  for the spectator;

(3) off-shell state: Gaussian momentum distribution of  $1 \text{ fm}^{-1}$  width for the pair and momentum  $q = \sqrt{4m(E + \epsilon_{\text{off}})}/3$  for the spectator.

These state types in the following will be indicated by superscripts “q”, “p”, and “off”, respectively, e.g., the state with  $p = 0, q = q_m, L = s = j = 0$  will be abbreviated by  $^1S_0^q$ .

### III. RESULTS

A number of force models are used for the present study of the  $3n$  system:

(1) A realistic high-precision charge-dependent Bonn (CD Bonn) potential [13] that was not applied to the  $3n$  system so far.

(2) A realistic Reid93 potential [14] already used in Ref. [7] where no physically observable  $3n$  resonance was found.

(3) Chiral effective field theory ( $\chi$ EFT) potential at next-to-leading order (NLO) [15], an improved version of the local NLO potential used in Ref. [4] that predicts a  $3n$  resonance about 1 MeV above threshold. The central value for the regulator  $R = 1.0 \text{ fm}$  is taken. The three-nucleon force (3NF) appears only at higher order but its contribution in multineutron systems is insignificant [4].

(4) A realistic Argonne V18 potential [16] whose low- and high-momentum components are partially decoupled by the similarity renormalization group (SRG) transformation [17, 18]. Taking the flow parameter  $\lambda = 1.8 \text{ fm}^{-1}$ , this model, without an explicit 3NF, reproduces quite well not only the  $^3\text{H}$  binding energy but also the cross section for  $n$ - $^3\text{H}$  scattering in the energy regime with pronounced four-nucleon resonances [19]. Thus, this particular SRG potential yields a better description of the  $3n + \text{proton}$  system and may be expected to provide more solid conclusions about the  $3n$  resonances as compared to other force models.

$3n$  transition matrix elements calculated with the above interactions show no indications of resonances. A common procedure is to vary the strength of the potential to generate an artificial resonance (or even a bound state) and to follow its evolution towards physical strength [4–7]. However, this way one may create also bound dineutron states, thereby introducing additional thresholds in the  $3n$  system that complicate the analysis. In fact, a

bound  $^1S_0$  dineutron appears already for the enhancement factor below 1.1 [7]. For this reason and since the  $^1S_0$  features are known quite well, the original potential is kept in the  $^1S_0$  partial wave while enhancing the potential strength in all higher waves by the same factor  $f$ , i.e.,

$$\langle p'L'sj|v|pLsj\rangle = \langle p'L'sj|v_{nn}|pLsj\rangle(\delta_{L'0}\delta_{L0} + f\bar{\delta}_{L'0}\bar{\delta}_{L0}) \quad (8)$$

where  $v_{nn}$  is the physical two-neutron potential. Bound dineutron appears in  $^3P_2 - ^3F_2$  ( $^3P_0$ ) partial wave at  $f = 7.24$  ( $f = 7.97$ ) when using the SRG model but at  $f = 4.0$  ( $f = 5.95$ ) when using the Reid93 model, the latter values being fully consistent with Ref. [7]. Although critical enhancement factors depend quite strongly on the potential model, the quantitative behavior of dineutron resonances, i.e., their trajectories in the complex energy plane, are quite similar: reducing  $f$  they acquire large width and for  $f = 1$  move deeply into the third quadrant becoming physically unobservable [7]. Such a behavior of dineutron resonances is fully consistent with Ref. [7] and is therefore not shown here.

I start a detailed  $3n$  system study with the  $J^\Pi = \frac{3}{2}^-$  state that was predicted in Ref. [4] to exhibit a resonance and in Ref. [7] to be the most favorable for the existence of bound trineutron when enhancing the  $nn$  interaction in the single  $^3P_2 - ^3F_2$  partial wave. In present work, unless explicitly stated otherwise, the  $nn$  interaction is enhanced in all partial waves with  $L \geq 1$  as given by Eq. (8). The SRG model produces a bound trineutron when  $f = 6.42$ . For lower  $f$  values a resonant behavior of  $T$  and  $U$  operators can be seen as demonstrated in Fig. 1 for several choices of initial and final channels of all three types described in previous section. If the two-neutron  $^1S_0$  state with vanishing relative momentum  $p = 0$  is interpreted as an unbound dineutron, the matrix element  $\langle ^1S_0^q|T_{J^\Pi}|^1S_0^q\rangle$  can be interpreted as the amplitude for “elastic” neutron-dineutron scattering. When the  $3n$  system energy approaches zero, this amplitude diverges as the driving term in Eq. (5) does due to kinematic reasons discussed in the previous section. This is not a resonance and it is not seen in other matrix elements of Fig. 1 where  $\langle ^3P_j^p|T_{J^\Pi}|^1S_0^q\rangle$  can be interpreted as the neutron-dineutron “breakup” amplitude in collinear kinematics [10, 11]. The off-shell matrix element  $\langle ^1S_0^{\text{off}}|U_{J^\Pi}|^1S_0^{\text{off}}\rangle$  shown in last panel of Fig. 1 has no direct physics interpretation. The most important message is that, if a given Hamiltonian supports a resonance, all matrix elements, despite their differences by several orders of magnitude or the repulsive character of the final-state interaction as in the  $^3P_1$  wave, as functions of energy exhibit resonant behavior corresponding to the same (within numerical accuracy) values  $E_r - i\Gamma/2$ . This is most evident for  $f = 6.2$  where the corresponding resonance at  $(1.41 - 0.22i)$  MeV is most pronounced. Decreasing  $f$  the pole moves to higher energy and away from the real axis; as a consequence, at  $f = 5.6$  with  $E_r - i\Gamma/2 = (4.36 - 2.24i)$  MeV the resonant behavior is far less pronounced. For the physical interaction strength

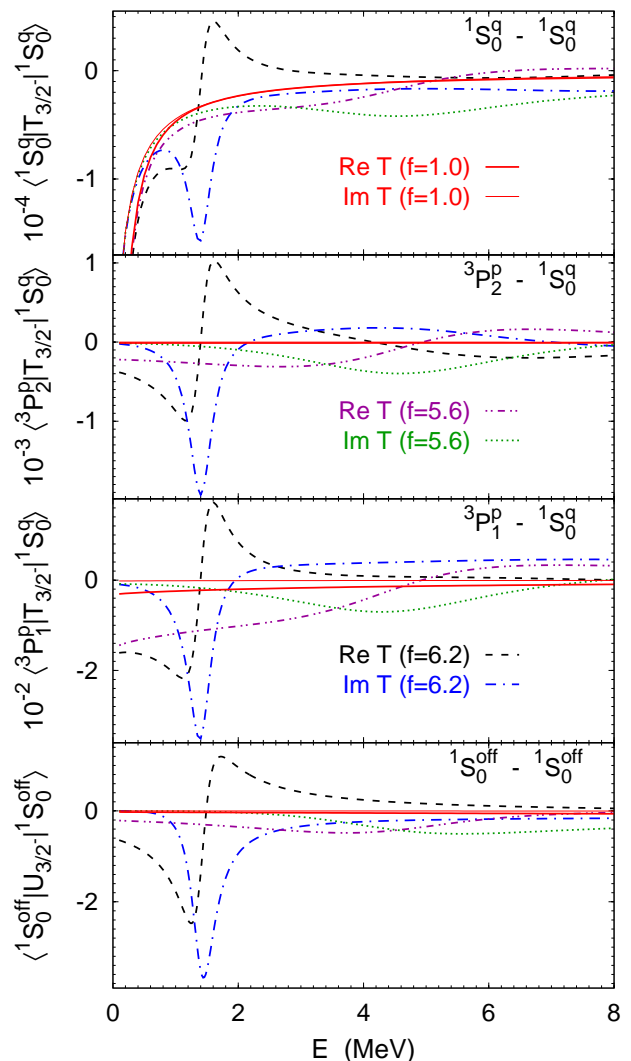


FIG. 1. (Color online) Energy dependence of real and imaginary parts of selected  $J^\Pi = \frac{3}{2}^-$  three-neutron transition matrix elements calculated using SRG potential with higher wave enhancement factors  $f = 1.0, 5.6$  and  $6.2$ . For the off-shell state  $\epsilon_{\text{off}} = 9$  MeV was chosen. Matrix elements are given in arbitrary units but preserving the relative scale.

$f = 1$  also shown in Fig. 1 by solid curves the resonant behavior can not be seen, and the magnitude of matrix elements is significantly smaller.

Transition strengths (probabilities) are proportional to squares of amplitudes; an example is shown in Fig. 2 for “breakup” transitions for the potential enhancement factor  $f$  ranging from 6.2 to 1. As expected, with decreasing  $f$  resonant peaks move to higher energy and become wider, disappearing around  $f = 4.0$ , i.e., well above the physical interaction strength  $f = 1$ . This fact strongly suggests the absence of physically observable  $3n$  resonance in the  $J^\Pi = \frac{3}{2}^-$  state, confirming the conclusions of Refs. [6, 7].

Further support for the above conclusion comes from

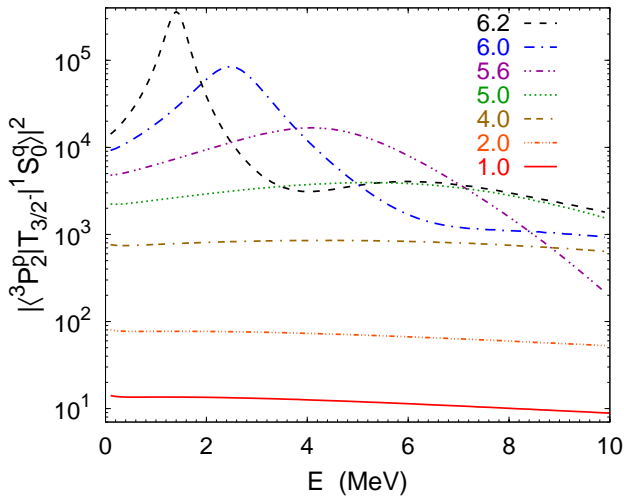


FIG. 2. (Color online) Energy dependence of transition strengths  $|\langle {}^3P_2^p | T_{3/2}^- | {}^1S_0^g \rangle|^2$  obtained using the SRG potential with higher-wave enhancement factors  $f = 6.2, 6.0, 5.6, 5.0, 4.0, 2.0,$  and  $1.0$ . Transition strengths are given in arbitrary units but preserving the relative scale.

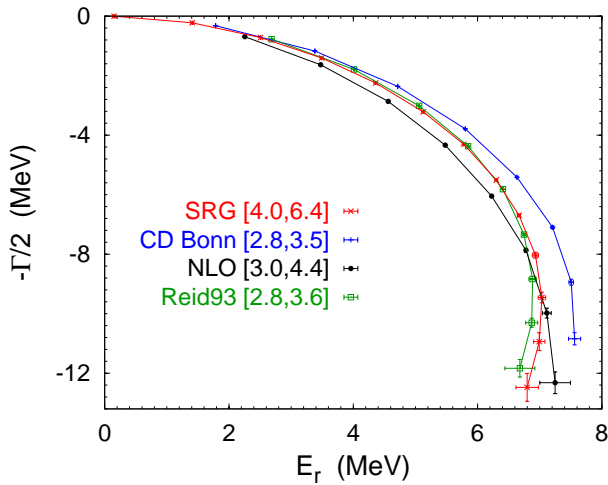


FIG. 3. (Color online) Three-neutron  $J^\Pi = \frac{3}{2}^-$  resonance trajectories for SRG, CD Bonn, NLO, and Reid93 potentials obtained varying the higher-wave (only  ${}^3P_2 - {}^3F_2$  for Reid93) enhancement factor  $f$  in the given interval with the step of  $0.1$  (CD Bonn and Reid93) or  $0.2$  (SRG and NLO). Lines are for guiding the eye only.

the Fig. 3 where the extracted  $J^\Pi = \frac{3}{2}^-$  transition operator pole trajectories in the complex energy plane are shown not only for SRG but also for CD Bonn, NLO, and Reid93 potentials. In the latter case, for the comparison with Ref. [7], the potential was enhanced in the  ${}^3P_2 - {}^3F_2$  wave only. The pole trajectory for Reid93 in Fig. 3 is in good agreement with the results of Ref. [7]. For soft potentials like NLO and, especially, SRG, the evolution with  $f$  is slower than for CD Bonn and Reid93. As

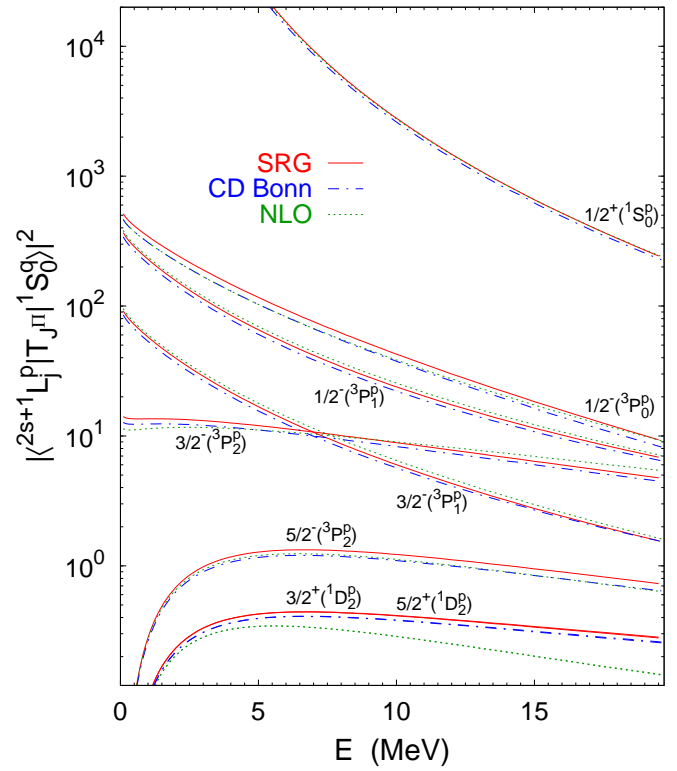


FIG. 4. (Color online) Energy dependence of transition strengths  $|\langle {}^{2s+1}L_J^p | T_{J\pi} | {}^1S_0^g \rangle|^2$  for  $J \leq \frac{5}{2}$  states obtained using physical SRG, CD Bonn, and NLO potentials. Transition strengths are given in arbitrary units but preserving the relative scale.  $\frac{3}{2}^+$  and  $\frac{5}{2}^+$  results are indistinguishable in the plot.

a consequence, NLO and SRG need larger  $f$  values to exhibit a  $3n$  resonance. Apart from that the trajectories are qualitatively similar for all potential models: decreasing the enhancement factor  $f$  the pole moves to higher energy and away from the real axis until the turning point  $E_r - i\Gamma/2 \approx (7 - 10i)$  MeV where  $E_r$  starts to decrease while  $\Gamma$  is rapidly increasing. Still, at this point  $f$  is around 3 or 4, indicating that the model system is far from the physical one with  $f = 1$ . Decreasing  $f$  below 3 or 4, depending on the potential, the pole moves too far from the real axis to be seen as a scattering resonance and its position therefore cannot be reliably extracted from  $3n$  transition operators calculated on the real axis. This fact is reflected in increased theoretical error bars, estimated from calculations with different initial and final states and with different number of terms (typically,  $n \leq 2$  to 4) in Eq. (7).

For the physical interaction strength  $f = 1$  no resonant behavior is seen also in other  $J^\Pi$  states. This is illustrated in Fig. 4 taking as example “breakup” transition strengths  $|\langle {}^{2s+1}L_J^p | T_{J\pi} | {}^1S_0^g \rangle|^2$  for all  $J \leq \frac{5}{2}$ . The results obtained with SRG, CD Bonn, and NLO potentials show some model dependence but all are consistent with the absence of an observable  $3n$  resonance. The

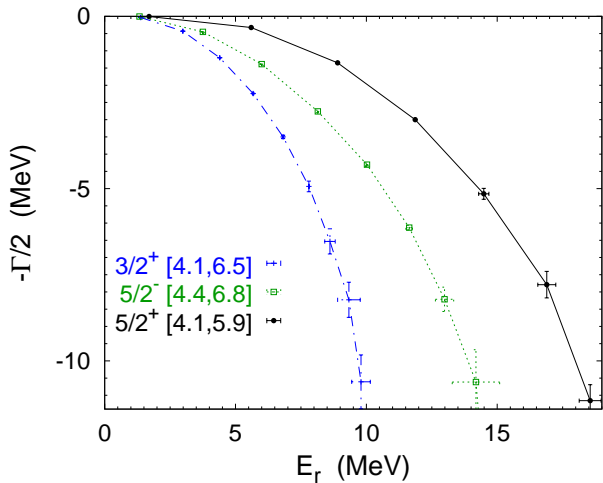


FIG. 5. (Color online) Three-neutron  $J^\Pi = \frac{3}{2}^+$ ,  $\frac{5}{2}^-$ , and  $\frac{5}{2}^+$  resonance trajectories for the SRG potential obtained varying the higher-wave enhancement factor  $f$  in the given interval with the step of 0.3. Lines are for guiding the eye only.

strongest transition strength seen in the  $J^\Pi = \frac{1}{2}^+$  state is mostly due to the final-state  $nn$   $t$ -matrix that acts in the  $^1S_0$  wave as compared to weaker  $P$  or  $D$  waves for other  $J^\Pi$  states. For vanishing energy this amplitude diverges as the corresponding driving term in Eq. (5) does, but it is not really resonant. In fact, in the considered  $nn$  interaction enhancement scheme the  $J^\Pi = \frac{1}{2}^\pm$  states are even less favorable for trineutron resonances than  $J^\Pi = \frac{3}{2}^\pm$  and  $J^\Pi = \frac{5}{2}^\pm$  states: At  $f = 7.24$ , with the bound  $^3P_2 - ^3F_2$  dineutron appearing in the SRG model,  $J^\Pi = \frac{1}{2}^\pm$  trineutrons are still not bound. In contrast, trineutrons in  $J^\Pi = \frac{3}{2}^+$ ,  $\frac{5}{2}^+$ , and  $\frac{5}{2}^-$  states become bound at  $f = 6.71$ , 6.02, and 6.94, respectively. Their pole trajectories when reducing the enhancement factor  $f$  are shown in Fig. 5. Qualitatively, the behavior is similar to the  $J^\Pi = \frac{3}{2}^-$  case of Fig. 3, but the real part  $E_r$  reaches higher values, especially for  $J^\Pi = \frac{5}{2}^+$ . Again, decreasing  $f$  below 4, the pole moves far away from the real axis and does not manifest itself as a visible scattering resonance.

Of course, resonance trajectories depend on the interaction enhancement scheme but the physical point  $f = 1$  is the same. In order to avoid the presence of bound dineutron, a different  $nn$  interaction enhancement scheme is used for the study of  $J^\Pi = \frac{1}{2}^\pm$  resonance trajectories: In the originally repulsive  $^3P_1$  partial wave the factor  $f$  in Eq. (8) is replaced by  $(2 - f)$  such that  $f = 1$  as before corresponds to the physical strength but the  $^3P_1$  potential becomes attractive with increasing  $f$ . In other waves the potential (8) is used. Using the SRG model in this scheme  $^3P_1$  dineutron becomes bound at  $f = 6.47$  while  $J^\Pi = \frac{1}{2}^+$ ,  $\frac{1}{2}^-$ , and  $\frac{3}{2}^-$  trineutrons become bound at  $f = 5.28$ , 5.48, and 5.44, respectively. Their resonance trajectories are shown in Fig. 6. Tra-

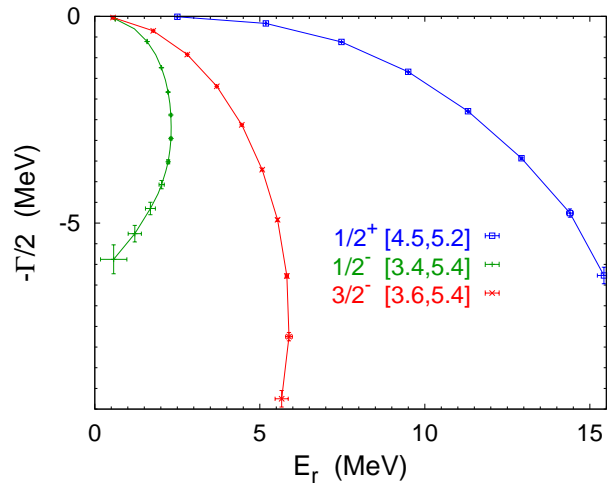


FIG. 6. (Color online) Three-neutron  $J^\Pi = \frac{1}{2}^+$ ,  $\frac{1}{2}^-$ , and  $\frac{3}{2}^-$  resonance trajectories obtained with the attractive  $^3P_1$  potential as described in the text. Results are based on the SRG model while the enhancement factor  $f$  is varied in the given interval with the step of 0.1 (0.2) for positive (negative) parity states.

jectories for  $J^\Pi = \frac{1}{2}^+$  and  $\frac{3}{2}^-$  are similar to those in Figs. 3 and 5 while the  $\frac{1}{2}^-$  trajectory stays much closer to the imaginary axis, i.e., the turning point is around  $E_r - i\Gamma/2 \approx (2.3 - 2.7i)$  MeV. Thus, the  $\frac{1}{2}^-$  resonance most evidently exhibits the trend to move to the  $E_r < 0$  region for  $f = 1$ , becoming physically unobservable.

An alternative approach to generate an artificial  $3n$  bound state or resonance is by adding an attractive  $3NF$ ; only the total isospin  $\frac{3}{2}$  component is acting in the  $3n$  system. However, the contribution of a realistic  $3NF$ , being of short range, is suppressed by the Pauli repulsion [2, 7], and unphysically strong  $3NF$  is needed to achieve a visible effect. Consistently with this observation, Ref. [4] found the effect of a realistic  $\chi$ EFT  $3NF$  in few-neutron systems to be very small. This suggests that the absence of an explicit  $3NF$  does not affect conclusions on the absence of the resonant behavior.

#### IV. CONCLUSIONS

The three-neutron system was studied using exact Faddeev-type equations for transition operators that were solved numerically in the momentum-space framework. Various on-shell and off-shell matrix elements were calculated searching for their poles in the complex energy plane leading to resonant behavior. An important advantage of the present transition operator approach as compared to previous bound-state-type studies is its ability to estimate not only the resonance position but also its effect on scattering amplitudes that include both resonant (if present) and nonresonant (also called back-

ground) contributions and their interference in collision observables. Since  $3n$  elastic scattering experiments are so far technically impossible, this work restricted itself to few selected transition strengths related to the  $3n$  collision process; this was sufficient to draw conclusions on  $3n$  resonances.

All tested physical  $nn$  force models, including the SRG potential successfully reproducing the resonant  $n$ - $^3\text{H}$  cross section, were found to exclude the possibility of an observable  $3n$  resonance. To generate artificial  $3n$  resonances (or even bound states) the  $nn$  interaction was enhanced in higher  $nn$  partial waves while keeping the original physical strength in the  $^1S_0$  partial wave. For appropriate (state  $J^\Pi$  and potential-dependent) enhancement factor values the resonant behavior was observed in all studied on-shell and off-shell matrix elements of  $3n$  transition operators. However, the resonant behavior disappears with the enhancement factor  $f$  still having a value around 3 or 4, i.e., for systems that cannot be considered as realistic  $3n$  systems. In these situations the resonance pole is typically more than 10 MeV away from the real axis while in transition amplitudes and strengths the background contribution dominates over the resonant one such that no resonant behavior can be seen. For this reason the transition operator pole trajectory in the complex energy plane could not be reliably followed towards

the physical limit  $f = 1$ , but it can be expected to be even further away from the real axis thereby excluding the physical observability of the  $3n$  resonance. This conclusion is fully consistent with Refs. [2, 6, 7] but contradicts Ref. [4]. The latter work, however, employed some questionable procedures such as the trineutron bound-state calculation above the dineutron threshold or the extrapolation of energy into a different sheet of the complex energy plane.

Despite the absence of resonant states, three-neutron transition amplitudes depend on the available energy and final state kinematics; thus, the existence of some peak structures in the transition strengths can not be excluded. In fact, the  $nn$  final-state interaction kinematics with vanishing two-neutron relative energy should correspond to a rather sharp peak due to the  $^1S_0$  virtual state as in the neutron-deuteron breakup [10, 11].

Given the controversy in the literature regarding the four-neutron resonance [2–5], the extension of the present transition operator study to the  $4n$  system is of high importance and interest. The work into this direction is underway.

The author acknowledges discussions with R. Lazauskas, the support by the Alexander von Humboldt Foundation under grant no. LTU-1185721-HFST-E, and the hospitality of the Ruhr-Universität Bochum where a part of this work was performed.

- 
- [1] K. Kisamori *et al.*, Phys. Rev. Lett. **116**, 052501 (2016).
  - [2] E. Hiyama, R. Lazauskas, J. Carbonell, and M. Kamimura, Phys. Rev. C **93**, 044004 (2016).
  - [3] A. M. Shirokov, G. Papadimitriou, A. I. Mazur, I. A. Mazur, R. Roth, and J. P. Vary, Phys. Rev. Lett. **117**, 182502 (2016).
  - [4] S. Gandolfi, H.-W. Hammer, P. Klos, J. E. Lynn, and A. Schwenk, Phys. Rev. Lett. **118**, 232501 (2017).
  - [5] K. Fosse, J. Rotureau, N. Michel, and M. Płoszajczak, Phys. Rev. Lett. **119**, 032501 (2017).
  - [6] A. Hemmdan, W. Glöckle, and H. Kamada, Phys. Rev. C **66**, 054001 (2002).
  - [7] R. Lazauskas and J. Carbonell, Phys. Rev. C **71**, 044004 (2005).
  - [8] E. O. Alt, P. Grassberger, and W. Sandhas, Nucl. Phys. **B2**, 167 (1967).
  - [9] Y. Koike, J. Haidenbauer, and W. Plessas, Phys. Rev. C **35**, 396 (1987).
  - [10] W. Glöckle, H. Witała, D. Hüber, H. Kamada, and J. Golak, Phys. Rep. **274**, 107 (1996).
  - [11] A. Deltuva, K. Chmielewski, and P. U. Sauer, Phys. Rev. C **67**, 034001 (2003).
  - [12] A. Deltuva, Ph.D. thesis, University of Hannover, 2003, <http://edok01.tib.uni-hannover.de/edoks/e01dh03/374454701.pdf>.
  - [13] R. Machleidt, Phys. Rev. C **63**, 024001 (2001).
  - [14] V. G. J. Stoks, R. A. M. Klomp, C. P. F. Terheggen, and J. J. de Swart, Phys. Rev. C **49**, 2950 (1994).
  - [15] E. Epelbaum, H. Krebs, and U.-G. Meißner, Phys. Rev. Lett. **115**, 122301 (2015).
  - [16] R. B. Wiringa, V. G. J. Stoks, and R. Schiavilla, Phys. Rev. C **51**, 38 (1995).
  - [17] S. K. Bogner, R. J. Furnstahl, and R. J. Perry, Phys. Rev. C **75**, 061001 (2007).
  - [18] S. K. Bogner, R. J. Furnstahl, A. Schwenk, and R. J. Perry, Phys. Lett. B **649**, 488 (2007).
  - [19] A. Deltuva, A. C. Fonseca, and S. K. Bogner, Phys. Rev. C **77**, 024002 (2008).